Blanquez-Casado *et al. EURASIP Journal on Wireless Communications and Networking* (2016) 2016:20
DOI 10.1186/s13638-016-0518-3

EURASIP Journal on Wireless Communications and Networking
a SpringerOpen Journal

RESEARCH Open Access

eOLLA: an enhanced outer loop link adaptation for cellular networks

Francisco Blanquez-Casado*, Gerardo Gomez, Maria del Carmen Aguayo-Torres and Jose Tomas Entrambasaguas

Abstract

Link adaptation (LA) process is a core feature for the downlink of 3GPP long-term evolution (LTE) and LTE-advanced (LTE-A). Through a channel quality indicator (CQI), the receiver suggests to the base station (BS) an appropriate modulation and coding scheme (MCS) according to the current channel conditions. In order to overcome any non-ideality in this process, the outer loop link adaptation (OLLA) algorithm is used to adaptively modify the mapping from signal-to-noise ratio (SNR) to CQI. OLLA basically modifies the measured SNR by an offset, according to whether data packets are received correctly or not, in order to adjust the average block error rate (aBLER) to a target. Although the OLLA technique has been extensively used, there exists a lack of analysis in the literature about its dynamics and convergence conditions. In this paper, a deep analysis of this algorithm has been carried out in order to cover this gap. From this analysis, we propose a new approach to the OLLA, the enhanced OLLA (eOLLA), which is able to adaptively modify its step size as well as to update its offset according to the reception conditions even if no data packets have been received. Thus, for LTE- and LTE-A-realistic scenarios, simulation results show that the proposed eOLLA outperforms the traditional OLLA, achieving a performance gain of up to a 15 % in terms of throughput.

Keywords: Link adaptation, AMC, LTE-A, OLLA, BLER

1 Introduction

The adaptive modulation and coding (AMC) process carried out in the link adaptation (LA) is a crucial part of current wireless communication systems. This technique allows to increase the data rate that can be reliably transmitted [1] and has been adopted as a core feature in cellular standards such as long-term evolution (LTE) and LTE-advanced (LTE-A) [2].

In the LTE and LTE-A downlink AMC procedure [2], the user equipment (UE) has to suggest to the base station (BS) an appropriate modulation and coding scheme (MCS) to be used in the next transmission in order to keep the block error rate (BLER) below a target. The proposed MCS is signaled from the UE by means of a channel quality indicator (CQI). Typically, each CQI is associated with a particular signal-to-noise ratio (SNR) interval; hence, MCSs are selected by mapping the estimated instantaneous SNR into its corresponding SNR interval, defined by an upper and a lower threshold.

*Correspondence: fbc@ic.uma.es
Department of Communications Engineering, Universidad de Málaga, Malaga, Spain

A static selection of the values for the AMC thresholds does not perform well in practical implementations as link conditions are inherently variant. It is usual to adjust these thresholds by means of the well-known outer loop link adaptation (OLLA) technique, which was first proposed in [3]. Basically, OLLA modifies the SNR thresholds by an offset [4, 5] which can be positive (making the MCS selection more robust) or negative (when the CQI selection was too strict). This offset is continuously updated based on the reliability of the received data blocks so that the average BLER is kept as close as possible to a predefined target.

Although there are works devoted to OLLA in the literature [6, 7], they typically address its performance from simulations, and the lack of a comprehensive analysis of its behavior in the literature is noticeable. Furthermore, to the best of our knowledge, previous works do not analyze the conditions under which the OLLA technique works properly. The first aim of this work is to cover this gap by carrying out a deep study of the OLLA technique.

From this study, improvements in the implementation of the traditional OLLA can be inferred. Thus, in this

paper, a different approach to the OLLA technique is proposed, the enhanced OLLA (eOLLA), which can significantly improve the performance of the traditional OLLA.

This paper is organized as follows. In Section 2, the AMC model for LTE used in this work is described, and then a detailed description of the OLLA is carried out, including a study of its convergence conditions and its performance. In Section 3, the proposed eOLLA is presented. Finally, Section 4 shows a comparison between both the traditional OLLA and the proposed eOLLA in realistic scenarios based on the downlink of LTE and LTE-A, and some concluding remarks are given in Section 5.

2 Outer loop link adaptation (OLLA)

To perform the AMC [1], the instantaneous SNR γ is estimated at the UE to determine the current fading region $\Re_i$ and, consequently, the transmission rate R_i (bits/symbol). At the UE, this instantaneous SNR is mapped into a certain CQI value, which is fed back to the BS.

The set of SNR thresholds $\{\Psi_i\}_{i=0,1,..,n}$ defines the intervals to map the estimated instantaneous SNR into its corresponding CQI, with Ψ_0 representing the minimum required SNR for transmission (outage condition) and $\Psi_n = \infty$. These thresholds have been designed in order to accomplish certain constraints, such as limiting the maximum instantaneous BLER (iBLER) or defining an average BLER (aBLER) target. The latter approach (based on aBLER) is the one adopted by most wireless technologies like LTE [1]. Therefore, our description will be focused on the aBLER scenario.

For a certain average SNR Γ, the average BLER under AMC can be evaluated as

$$aBLER(\Gamma, \{\Psi_i\}) = \sum_{i=0}^{n-1} \int_{\Psi_i}^{\Psi_{i+1}} iBLER_i^{AWGN}(\gamma) p^o(\Gamma, \gamma) d\gamma, \tag{1}$$

being $iBLER_i^{AWGN}(\gamma)$, the instantaneous BLER for a given MCS i over an additive white Gaussian noise (AWGN) channel and $p^o(\Gamma, \gamma)$ the probability density function (PDF) of the instantaneous SNR conditioned to transmission.

In this, work we have assumed an uncorrelated Rayleigh channel for the analysis. Thus, the PDF of the instantaneous SNR for a certain average SNR Γ is given by an exponential function [1]

$$p(\Gamma, \gamma) = \frac{1}{\Gamma} e^{-\gamma/\Gamma}. \tag{2}$$

Then, the instantaneous SNR conditioned to transmission is given by:

$$p^o(\Gamma, \gamma) = \begin{cases} \frac{1}{A(\Gamma, \Psi_0)\Gamma} e^{-\gamma/\Gamma}, \gamma > \Psi_0 \\ 0, \text{else} \end{cases} \tag{3}$$

where $A(\Gamma, \Psi_0)$ is the probability of not being in outage, that is,

$$A(\Psi_0) = \int_{\gamma=\Psi_0}^{\infty} \frac{1}{\Gamma} e^{-\gamma/\Gamma} d\gamma = e^{-\Psi_0/\Gamma}. \tag{4}$$

According to Eq. (1), in order to evaluate the aBLER, it is necessary to have at our disposal an expression for $iBLER_i^{AWGN}$, but to the best of our knowledge, this is not available in the literature when turbo coding is used. Moreover, the exact value of the iBLER strongly depends on the specific decoder implementation [8]. Nevertheless, since the iBLER metric represents the probability of being in one of two states $\{error, no - error\}$, we propose the use of binary logistic regression [9]. This regression is a binary classifier based on one or more input variables. Thus, it is a useful tool to model iBLER curves for each MCS i over AWGN channels, for a given instantaneous SNR γ, by means of binary logistic functions as:

$$iBLER_i^{AWGN}(\gamma) \approx f_i(\gamma) = \frac{1}{1 + e^{-\alpha_{i_0}\gamma - \alpha_{i_1}}}, \tag{5}$$

where the α_{i_0} and α_{i_1} values (see Table 1) are to be found from the logistic regression over results of the actual decoder implementation (see Section 3.2 for further details). The accuracy of logistic functions after the curve-fitting process is shown in Fig. 1 for the whole set of CQI values of LTE [2], where solid lines represent the analytic BLER curves whereas simulation results of a soft output Viterbi algorithm (SOVA)-based turbo decoder [10] are marked with circles.

A static selection of the values for the AMC thresholds Ψ_i does not perfectly adjust the aBLER to a target since link conditions are inherently variant. Thus, in order

Table 1 Values of α_{i_0} and α_{i_1} of modeled iBLER curves

CQI index	α_{i_0}	α_{i_1}
1	−28.08	9.71
2	−20.59	11.05
3	−15.31	12.89
4	−11.09	14.45
5	−8.05	17.12
6	−6.56	20.56
7	−2.48	16.07
8	−2.39	22.83
9	−1.26	18.74
10	−0.67	20.02
11	−0.40	18.36
12	−0.26	16.62
13	−0.17	16.18
14	−0.04	7.02
15	−0.03	8.84

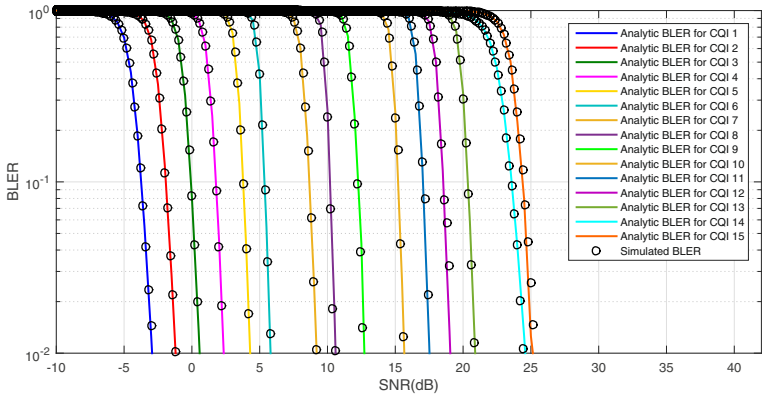

Fig. 1 Curve fitting of logistic functions to model iBLER curves (CQIs 1–15)

to meet the $aBLER_T$, different sets of SNR thresholds $\{\Psi_i\}_{i=0,1,..,n}$ should be used for different link conditions. This can be modeled by rewriting each SNR threshold $\Psi_i = \gamma_i \cdot \theta$, being γ_i an initial value, and θ an offset that must be designed to meet the $aBLER_T$. Then, Eq. (1) is modified as

$$aBLER(\Gamma, \{\gamma_i\}, \theta) = \sum_{i=0}^{n-1} \int_{\gamma_i \theta}^{\gamma_{i+1} \theta} iBLER_i^{AWGN}(\gamma) p(\gamma) d\gamma. \tag{6}$$

The previous process is typically performed in practical implementations by the outer loop link adaptation (OLLA) technique [3–5]. The traditional OLLA operation consists in dynamically modifying the value of the offset according to whether the previously transmitted data packet has been correctly received or not. In LTE and LTE-A, this information is extracted from the cyclic redundancy code (CRC) [11]. Thus, OLLA can be seen as a discrete time system in which, each time k a CRC is received, the value of the offset $\theta[k]$ is updated according to the following equation [5]

$$\theta_{dB}[k] = \theta_{dB}[k-1] + \Delta_{up} \cdot e[k] - \Delta_{down} \cdot (1 - e[k]), \tag{7}$$

being

- $\theta_{dB}[k] = 10 \cdot log_{10}(\theta[k])$.
- $e[k]$ an error indicator, whose value is 0 if the CRC is correct, or 1 if not. It corresponds to a dichotomous random variable whose average is the aBLER.
- Δ_{up} and Δ_{down} constant increment and reduction values, respectively, of the offset, in decibels. These two values are positive and should satisfy Eq. (8) in order to meet the $aBLER_T$ [5]. This condition will be justified in Subsection 2.1.

$$aBLER_T = \frac{1}{1 + \frac{\Delta_{up}}{\Delta_{down}}}. \tag{8}$$

In addition to that, the value of Δ_{down} cannot exceed an upper limit $\Delta_{down_{max}}$ in order to ensure the proper working of the OLLA. This limit is given by the next equation, which is justified in Subsection 2.1.

$$\Delta_{down_{max}} < \frac{2e \cdot aBLER_T}{-\alpha_1}. \tag{9}$$

SNR threshold values are now modified at each instant k by a discrete offset, so they can be expressed as

$$\Psi_i[k] = \gamma_i \cdot \theta[k]. \tag{10}$$

To sum up, the OLLA operation consists in increasing the offset value (and so increasing the value of the SNR thresholds) when error happens, and decreasing them when transmissions are correct. Therefore, $\theta[k]$ values higher than 1 increase transmission robustness, while values lower than 1 decrease it.

2.1 OLLA convergence in average

It should be noticed that OLLA dynamics imply that the offset value $\theta_{dB}[k]$ is continuously being updated by adding Δ_{up} (if error) or subtracting Δ_{down} (if not). Thus, it will never converge to a single value. However, the offset θ presented in (6) is a single value that ensures the $aBLER_T$ for stationary link conditions. The reason of this difference is that θ is used in an averaging process, while in case of the OLLA, $\theta_{dB}[k]$ is an instantaneous value. Therefore, to study the convergence of the OLLA process, averaged values must be considered.

In this subsection, the convergence in average of the OLLA algorithm for stationary link conditions, as well as the conditions that should be satisfied in order to achieve this convergence is studied. For this purpose, mathematical expectation can be applied to (7) to find the averaged

$E[\theta_{dB}[k]] = \theta_{dB_k}$ value at k, obtaining the following equation after reordering

$$\theta_{dB_k} = \theta_{dB_{k-1}} + \left(\Delta_{up} + \Delta_{down}\right) \cdot E[e[k]] - \Delta_{down}. \quad (11)$$

Note that since the average value of $\theta_{dB}[k]$ depends on k, it is not an ergodic process. Only when $k \to \infty$ the process can be considered ergodic. Expression (11) corresponds to a difference equation, i.e., there is a recurrence relation between the terms in the form of $\theta_{dB_k} = T\left(\theta_{dB_{k-1}}\right)$, being $T(\theta_{dB})$ the recurrence function. Hence, according to the Banach fixed-point theorem [12], when $k \to \infty$ the equation will converge to the only value such that $\theta^o_{dB} = T\left(\theta^o_{dB}\right)$ if certain conditions are fulfilled. The following equation is obtained when convergence in average is reached

$$\left(\Delta_{up} + \Delta_{down}\right) \cdot E[e[k]] - \Delta_{down} = 0. \quad (12)$$

Note that $E[e[k]]$ is the average number of errors, i.e., the aBLER. Thus, in order to ensure that the converged offset value $\theta^o_{dB} = 10 \cdot log_{10}(\theta^o)$ meets the $aBLER_T$, the aBLER should be forced to this value, obtaining the the following relation

$$aBLER_T = E[e[k]] = \frac{1}{1 + \frac{\Delta_{up}}{\Delta_{down}}}. \quad (13)$$

which was already presented in (8), and now it has been justified. Therefore, under certain link conditions, the OLLA algorithm converges in average to a value θ^o which is the value of θ to be introduced in (6) in order to meet the $aBLER_T$.

Equation (13) manifests that there are infinite suitable combinations of Δ_{up} and Δ_{down} that ensures the $aBLER_T$. However, the specific values of Δ_{up} and Δ_{down} must accomplish the convergence criteria required by the Banach fixed-point theorem applied to (11), whose two sufficient conditions are described next.

2.1.1 First Banach fixed-point theorem condition

The function $T(\theta_{dB})$ should be a contraction mapping, that is, it should satisfy that

$$T(\theta_{dB}) \in [\theta_{min}, \theta_{max}], \forall \theta_{dB} \in [\theta_{min}, \theta_{max}]. \quad (14)$$

It can be easily shown that this condition is always fulfilled by the OLLA. Firstly, since $E[e[k]]$ is the average number of errors, i.e., the aBLER, its range of values are comprised between 0 and 1. Thus, there will be a value $\theta_{dB} = \theta_{min}$ low enough to ensure that $\mathrm{E}[e[k]] = 1$, which means that $T(\theta_{min}) = \theta_{min} + \Delta_{up}$. Then, as θ_{dB} increases, the value of $\mathrm{E}[e[k]]$ will decrease until θ_{dB} raises a value θ_{max} high enough to ensure that $\mathrm{E}[e[k]] = 0$, which means that $T(\theta_{max}) = \theta_{max} - \Delta_{down}$. As a result of that, the values of $T(\theta_{dB})$ will be comprised between

$$T(\theta_{dB}) \in \left[\theta_{min} + \Delta_{up}, \theta_{max} - \Delta_{down}\right] \in [\theta_{min}, \theta_{max}], \forall \theta_{dB} \in [\theta_{min}, \theta_{max}]. \quad (15)$$

2.1.2 Second Banach fixed-point theorem condition

The second condition that the function $T(\theta_{dB})$ should fulfill is that

$$\left|T'(\theta_{dB})\right| < 1, \ \forall \theta_{dB} \in [\theta_{min}, \theta_{max}] \quad (16)$$

being $T'(\theta_{dB})$ the first order derivative of $T(\theta_{dB})$. To check this condition, it is necessary as an expression for $\mathrm{E}[e[k]]$, this is, for the aBLER. This expression is provided by (6), and it depends on the specific parameters of the binary logistic regression carried out to model the $iBLER_i^{AWGN}$ curves. In order to have a more tractable expression, $aBLER(\Gamma, \{\gamma_i\}, \theta)$ values have been obtained numerically for an average SNR value of $\Gamma = 15dB$ and certain $iBLER_i^{AWGN}$ curves (see Section 5 for further details) for different θ_{dB} values according to (3), (5), and (6). These values have been obtained based on the parameters of Table 2 and are presented in Fig. 2 (solid line).

The shape of the aBLER curve is similar to the iBLER. Thus, it could also be modeled by means of logistic regression, which was introduced in Section 2. In this case, we propose to model this curve by means of a modified binary logistic function, which introduces a parameter s which controls the slope, as

$$E[e[k]] = aBLER(\Gamma, \theta_{dB}) \approx f_m(\theta_{dB}) = \frac{1}{\left(1 + e^{-\alpha_0 \theta_{dB} - \alpha_1}\right)^s}. \quad (17)$$

After finding the values of α_0, α_1, and s by logistic regression, the resulting fitted curve is shown in Fig. 2 as a dashed line. It can be seen how the proposed expression perfectly fits with the simulated results.

By using the proposed modified logistic function, it can be evaluated by the expression of $T(\theta_{dB})$, according to (11), as

$$T(\theta_{dB}) = \theta_{dB} + \left(\Delta_{up} + \Delta_{down}\right) \cdot f_m(\theta_{dB}) - \Delta_{down} \quad (18)$$

Next, the condition to ensure that $\left|T'(\theta_{dB})\right| < 1$ is derived from (13), (17), and (18). First, we find the value of $T'(\theta_{dB})$ as

Table 2 Parameters for OLLA convergence

Parameter	Value
Γ	15 dB
α_0	1.15
α_1	−1.03
s	17
$\Delta_{down_{max}}$	0.52
$aBLER_T$	0.1

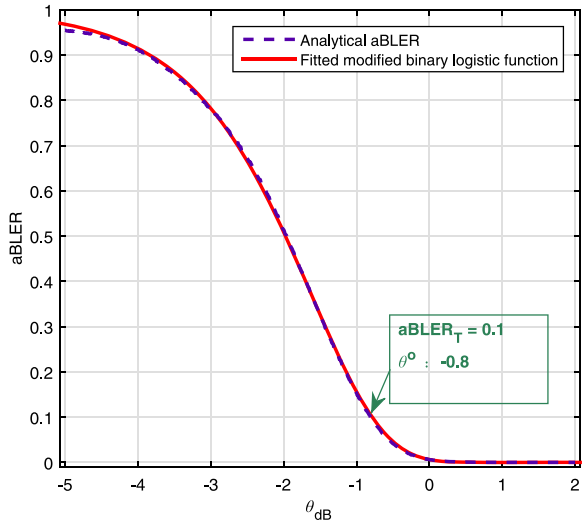

Fig. 2 Curve fitting of modified logistic function to model aBLER for $\Gamma = 15$ dB

$$T'(\theta_{dB}) = 1 + (\Delta_{up} + \Delta_{down}) \cdot f'_m(\theta_{dB}). \quad (19)$$

Since $f_m(\theta_{dB})$ is a decreasing function, that is $f'_m(\theta_{dB}) \leq 0$, and both Δ_{up} and Δ_{down} are positive, the following condition must be guaranteed in order to ensure the convergence condition

$$(\Delta_{up} + \Delta_{down}) \cdot |f'_m(\theta_{dB})| < 2 \Rightarrow |f'_m(\theta_{dB})| < \frac{2}{(\Delta_{up} + \Delta_{down})}. \quad (20)$$

Thus, we find the maximum of $|f'_m(\theta_{dB})|$, i.e., the values for which $f''_m(\theta_{dB}) = 0$, to ensure that the condition imposed by (20) is fulfilled. After reordering, we find that the offset value $\theta_{dB_{max}}$ for which the maximum of $|f'_m(\theta_{dB})|$ is achieved as

$$\theta_{dB_{\max}} = \frac{1}{\alpha_1} \cdot \left(\ln \left(\frac{1}{s} + \alpha_0 \right) \right) \quad (21)$$

and therefore, the maximum value of $|f'_m(\theta_{dB})|$ is

$$|f'_m(\theta_{dB_{\max}})| = |\alpha_1| \cdot \frac{1}{(1 + 1/s)^{s+1}}. \quad (22)$$

As it was said before, the fact that $f_m(\theta_{dB})$ is a decreasing function implies that $s \geq 0$. It can be easily seen that higher values of $f_m(\theta_{dB})$ are achieved as s is increased. Then, we get an upper bound of $f'_m(\theta_{dB})$ when $s \to \infty$ as

$$|f'_{m_{\max}}| = \frac{|\alpha_1|}{e}. \quad (23)$$

Finally, from (13), (20), and (23), we find that the second condition to ensure the OLLA convergence, which was already presented in (9), is given by

$$\Delta_{down_{max}} < \frac{2e \cdot aBLER_T}{-\alpha_1}.$$

Thus, convergence is ensured if the decrement step does not raise a maximum value, which is determined by α_1, that is, by the curve of aBLER for a certain Γ value of mean SNR.

According to previous results, there is a range of Δ_{down} values, and so of Δ_{up} values, that ensures convergence. In Fig. 3, the convergence process when different values of Δ_{down} are used is presented, for given link conditions whose parameters are listed in Table 2. These parameters have been obtained for the same conditions in Fig. 2.

Figure 3, shows how the converged value θ_{dB_k} raises its final value $\theta^o_{dB} \approx -0.8$ (dashed line) faster as the size of

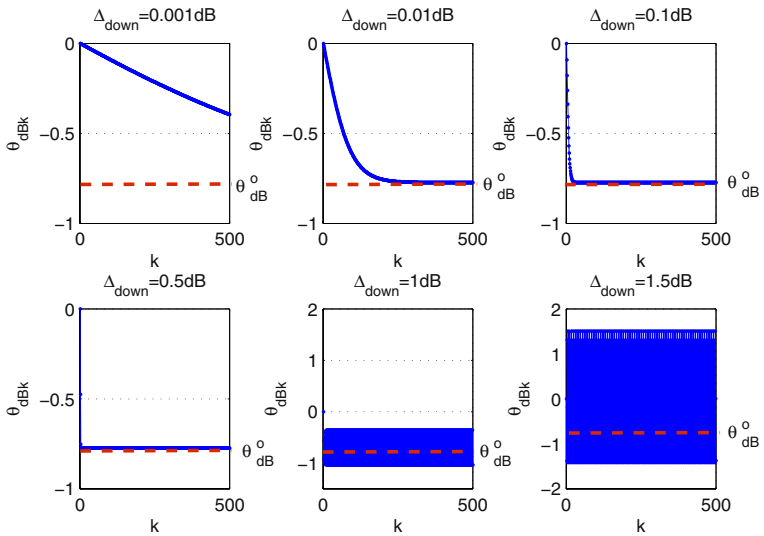

Fig. 3 OLLA convergence in average for different Δ_{down} values; $aBLER_t = 0.1$

Δ_{down} is higher. Note that this convergence value is the same that obtained in Fig. 2 by using (17). Once Δ_{down} exceeds $\Delta_{down_{max}}$, whose value is 0.52 for the proposed scenario, the OLLA begins to diverge, this divergence being more remarkable as Δ_{down} increases. Therefore, it would be advisable to choose the highest possible value of Δ_{down} in order to achieve convergence as fast as possible.

2.2 OLLA performance

In this subsection, the OLLA performance is analyzed under stationary link conditions. As it will be shown, when convergence, the instantaneous offset value $\theta_{dB}[k]$ fluctuates around the converged value θ^o_{dB} following the instantaneous channel variations. The amplitude of these fluctuations will be related to the values of Δ_{up} and Δ_{down}. Thus, high values of these two parameters, even if they guarantee the OLLA convergence, may lead to a high variance in the instantaneous offset value that could degrade the OLLA performance. On the other hand, too small values of Δ_{up} and Δ_{down} may imply that the OLLA could not follow the channel variations if they are too fast.

In Fig. 4, the instantaneous values of $\theta[k]$ are shown for the same simulation conditions of Table 2, for a set of values of Δ_{down} that guarantee convergence ($\Delta_{down} < \Delta_{down_{max}} = 0.52$). These results show that for the lowest Δ_{down} value, it takes several steps to the OLLA to reach a state for which the offset is stabilized around a certain value, which is the converged value $\theta^o_{dB} \approx -0.8$ of Fig. 3. As the value of Δ_{down} increases, it takes less steps to the OLLA to stabilize; however, the variance of the offset also increases, which may cause a degradation in the OLLA performance.

As it was previously stated, a high variance of the OLLA offset can degrade its performance. This fact is shown in Table 3, which presents the achieved throughput and

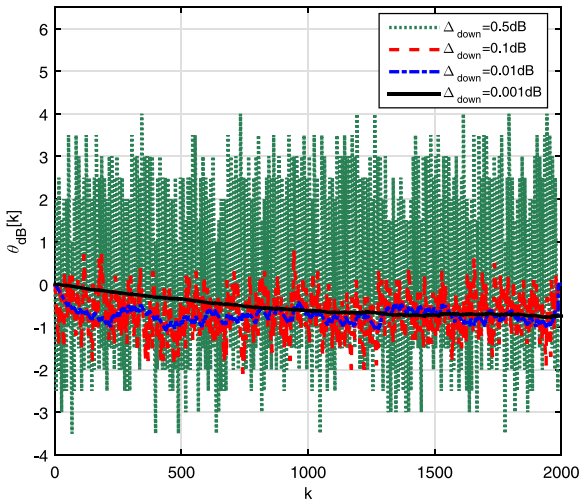

Fig. 4 Instantaneous offset for an uncorrelated flat Rayleigh channel

Table 3 System performance for OLLA with different Δ_{down} sizes

Δ_{down} size (dB)	Spectral efficiency (bps/Hz)	aBLER
0.001	2.98	0.1
0.01	3	0.1
0.1	2.96	0.1
0.5	2.76	0.1

the aBLER for the different Δ_{down} values, under the same condition as in Fig. 4. Results reveal that as the size of the step increases, there is a reduction of the spectral efficiency, although all configurations meet the $aBLER_T$. The reduction of spectral efficiency for the maximum Δ_{down} value that guarantees convergence (0.5 dB) is about 8 % with respect to the step value with better throughput performance ($\Delta_{down} = 0.01$ dB).

The reason for this throughput degradation for high step values is that they may cause that when an error happens, the OLLA selects a more robust MCS than the required to ensure the $aBLER_T$.

To sum up, while high values of the OLLA steps are desirable to achieve a fast convergence, low step values lead to higher throughput once convergence is achieved, since it provides a better adjustment of the MCS. Thus, the selection of the values of Δ_{up} and Δ_{down} should be carried out carefully in order to optimize the OLLA performance.

3 Enhanced outer loop link adaptation

In the previous section, the traditional OLLA algorithm has been deeply studied, showing that a key factor to optimize the performance is the appropriate selection of its step size. However, the way this selection should be carried out is not clear. Moreover, the performance of the OLLA also depends on the specific implementation of features at the receiver such as the turbo decoder or the channel estimation method.

In addition to that, another problem is that the OLLA only updates its offset every time k an ACK/NACK is received, i.e., when a transmission is done. In real scenarios, it is usual not to have full-buffer traffic but a discontinuous transmission with variable traffic. In these cases, the UE may be most of the time in idle mode [13]. Therefore, a combination of variant channel conditions together with these kind of traffic patterns could cause a performance degradation since the OLLA may not be able to update its offset fast enough to follow the channel variations.

3.1 Proposed eOLLA

In this section, we propose a modification of the traditional OLLA algorithm, the enhanced outer loop link adaptation (eOLLA), which is able to adapt the size of the steps according to the convergence status of the

system. Furthermore, the proposed eOLLA updates its offset independently of whether a transmission is carried out or not.

Since the error indicator $e[k]$ used in the traditional OLLA can be seen as a one bit instantaneous BLER estimator (1 if error, 0 if not), this value could be replaced by a more accurate instantaneous BLER estimation. Thus, to carry out the implementation of the proposed eOLLA, a model for the instantaneous BLER of each MCS i over AWGN channels for instantaneous SNR, $iBLER_i^{AWGN}(\gamma)$, is needed.

The proposed eOLLA implemented from (7) is as follows

1. If an ACK/NACK is received, update the corresponding $iBLER_i^{AWGN}$ model according to the MCS i used in this transmission (optional).
2. Estimate the instantaneous SNR value $\gamma[t]$.
3. At each Transmission Time Interval (TTI) t, calculate the instantaneous BLER value $B[t] = iBLER_i^{AWGN}(\gamma[t])$.
4. Get the offset value as

$$\theta_{dB}[t] = \theta_{dB}[t-1] + \Delta_{up} \cdot B[t] - \Delta_{down} \cdot (1 - B[t]). \quad (24)$$

In the eOLLA algorithm description, it should be noticed that the index k of Eq. (7) of the traditional OLLA description has been replaced by the index t in Eq. (24). This means that the offset of the eOLLA will be updated every TTI t (every time a transmission can be potentially carried out) instead of every time k a CRC is received (every time a transmission is carried out). Then, in case of discontinuous transmissions, the proposed eOLLA updates its offset more frequently than in case of the traditional OLLA, which implies that the eOLLA is able to follow easily the temporal variations of the channel, thus improving the AMC performance.

This continuous updating of the eOLLA offset can be easily performed in LTE since there is an estimation of the SNR available every TTI t. In the downlink of LTE and LTE-A, the BS transmits reference signals (RS) [2] at each subframe, in both connected and idle modes. Thus, every UE is able to perform SNR estimation from this RS at each TTI, and so to update its eOLLA offset.

The fitting process referred in step (1) of the proposed algorithm is used to adjust the instantaneous BLER model to the specific system implementation used. This process is required just in case a fitted model is not available.

For the purpose of a better understanding of the eOLLA behavior, step (4) can be rewritten according to (13) as

$$\theta_{dB}[t] = \theta_{dB}[t-1] + \Delta_{down} \cdot \left(\frac{B[t]}{aBLER_T} - 1 \right). \quad (25)$$

From the previous equation, it can be deduced that the proposed eOLLA adapts the increment to be applied to the offset according to the difference between the estimated instantaneous BLER $B[t]$ and the target aBLER. Then, if $B[t] = 0$, the offset will be decreased by Δ_{down}, thus decreasing the robustness of the next transmission in the same way than in the traditional OLLA. As $B[t]$ increases, the size of the decreasing step reduces, and so increases the robustness of the next transmission until $B[t] = aBLER_T$, which is the equilibrium point. At this point, no step will be applied to the offset, since if the eOLLA remains in this state the average BLER will meet the target aBLER. In case that $B[t]$ exceeds the $aBLER_T$, the offset will be increased, and thus the robustness of the next transmission, until $B[t] = 1$. In this case, the offset will be increased by Δ_{up}, as in the traditional OLLA.

Hence, for the eOLLA, if the offset value leads to either a very high or a very low instantaneous BLER, high-step values are used in order to correct this situation as fast as possible. Then, as the iBLER is closer to the average target BLER, lower step sizes are used to reduce the variance of the MCS and maximize the throughput.

Since $E[B[t]]$ is the same than $E[e[t]]$, the convergence analysis of the traditional OLLA carried out in Subsection 2.1 can be applied to the eOLLA. Thus, to ensure the convergence of the eOLLA, condition (9) must be also satisfied. Note that under stationary conditions, the offset value for which $E[B[t]] = aBLER_T$ corresponds to the convergence value θ_{dB}^o previously described.

3.2 Logistic regression implementation

In previous section, we stated that an expression of the instantaneous BLER $iBLER_i^{AWGN}(\gamma[t])$ was required to model the eOLLA algorithm. As described in Section 2, instantaneous BLER for MCS i over AWGN channels can be modeled by means of binary logistic functions.

Therefore, logistic regression can be used in the eOLLA algorithm (step 1) to find out the values of α_{i_0} and α_{i_1} in Eq. (5) that better fit with the $iBLER_i^{AWGN}$ curve. In practice, this logistic regression can be easily implemented by the well-known gradient descend algorithm [14]. This algorithm is typically used to minimize a cost function $J(\alpha)$ as follows

$$\alpha := \alpha - \lambda \frac{\partial}{\partial \alpha} J(\alpha) \quad (26)$$

where λ is a parameter that controls the convergence speed. Thus, first of all, it is necessary to provide the logistic regression cost function, given by [15]

$$J(\alpha) = y \cdot \log\left(f_\alpha(x)\right) - (1-y) \cdot \log\left(1 - f_\alpha(x)\right) \quad (27)$$

being x, the input to the system, y, the class the input x falls into (with only two possible values, 0 or 1), and f_α a binary logistic function to model the mapping of x into a class y. Thus, to translate the generic logistic regression function to our problem, we associate the input x to the

instantaneous SNR value γ, the classification result y as an error indicator e, and f_α as the binary logistic function of (5). Then, applying partial derivation of the cost function, the resulting logistic regression process for the proposed eOLLA is given by:

$$\begin{cases} \alpha_{i_0}^k = \alpha_{i_0}^{k-1} - \lambda \cdot \left(\frac{1}{1+e^{-\alpha_{i_0}^{k-1} - \alpha_{i1}^{k-1} \cdot \gamma[k-1]}} - e[k] \right) \\ \alpha_{i_1}^k = \alpha_{i_1}^{k-1} - \lambda \cdot \left(\frac{1}{1+e^{-\alpha_{i_0}^{k-1} - \alpha_{i1}^{k-1} \cdot \gamma[k-1]}} - e[k] \right) \cdot \gamma[t-1], \end{cases} \tag{28}$$

where $e[k]$ is, as in (7), an error indicator of the received packet at the instant k, which is obtained from the ACK/NACK report, and $\gamma[t-1]$ is the estimated instantaneous SNR during the previous TTI t. Note that the values of $\alpha_{i_0}^k$ and $\alpha_{i_1}^k$ have to be updated simultaneously. Regarding λ, low values will lead to a slower but a more accurate convergence, while high values will accelerate the convergence, although it may also cause oscillations. However, it should be noticed that the logistic regression cost function is convex, so convergence is guaranteed.

3.3 eOLLA performance

Figure 5 shows the instantaneous offset value $\theta[t]$ of the eOLLA for the same conditions as that in Fig. 4. Note that in this case, $t = k$ since a transmission is carried out every TTI. In this figure, it can be seen that the convergence values are the same with that achieved for the traditional OLLA. In addition, instantaneous offset values have lower variance than the ones obtained in Fig. 4 for the same Δ_{down}.

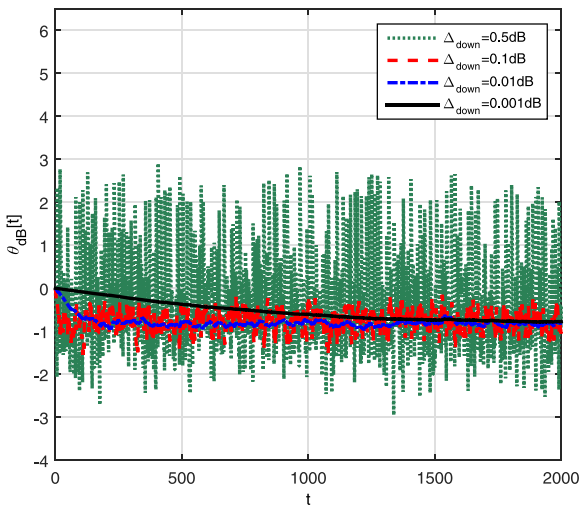

Fig. 5 Instantaneous offset for an uncorrelated flat Rayleigh channel

Throughput and aBLER results are shown in Table 4. For the eOLLA, an increment of Δ_{down} does not lead to an important throughput degradation as in the case of the traditional OLLA (see Table 3). The throughput degradation when using the highest Δ_{down} considered in these simulations is about 4 % for the eOLLA, while for the traditional OLLA, this degradation is doubled. In both cases, the $aBLER_T$ is met.

Results presented for the traditional OLLA and the eOLLA do not correspond to a realistic scenario, since an uncorrelated channel is assumed. However, they are useful in order to understand the dynamics of both the OLLA and the proposed eOLLA. In practice, AMC cannot be used in uncorrelated channels due to the outdating of CQI reports. Next, both OLLA and eOLLA have been evaluated in a correlated channel scenario. Furthermore, a bursty traffic pattern has been taken into account in order to give a complete picture.

Figure 6 shows the instantaneous offset values for both the traditional OLLA and the eOLLA for a correlated flat Rayleigh channel with a Doppler frequency (f_D) of 7 Hz and $aBLER_T = 0.1$, when a small Δ_{down} step is used (0.001 dB). The transmission periods are expressed in percentage of the maximum traffic load case. First of all, notice that the same results are achieved by the eOLLA independently of the traffic load, since the eOLLA only needs the estimated iBLER (available at each TTI) to update the offset. In contrast, different performance is achieved by the traditional OLLA depending on the traffic load, since it needs an ACK/NACK report to update its state. As a consequence, when full buffer is assumed, i.e., $t = k$, both OLLA implementations have a similar performance; but as the traffic load decreases, it is harder for the traditional OLLA to follow the temporal channel variations since its offset is only updated when a CRC is received, thus degrading its performance compared to the eOLLA, which updates its offset every TTI.

On the other hand, if the same simulation is carried out with a high step size $\Delta_{down} = 0.5$, which ensures convergence, this convergence is easily achieved independently of the traffic load. However, low load is still a problem for the traditional OLLA since it is not able to properly follow the channel, as shown in Fig. 7.

Table 4 System performance for eOLLA with different Δ_{down} sizes

Δ_{down} size (dB)	Spectral efficiency (bps/Hz)	aBLER
0.001	2.99	0.1
0.01	3	0.1
0.1	2.99	0.1
0.5	2.89	0.1

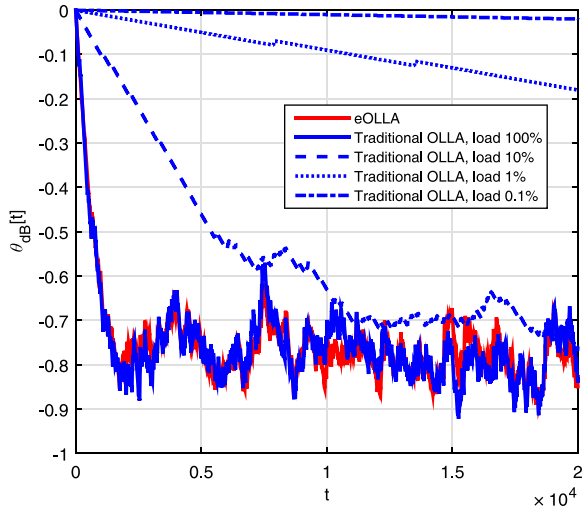

Fig. 6 Instantaneous offset comparison for a correlated flat Rayleigh channel ($f_D = 7$ Hz) with $\Delta_{down} = 0.001$ dB

Table 5 summarizes the spectral efficiency results for different traffic loads and Δ_{down} sizes for both the traditional OLLA and the eOLLA, assuming $aBLER_T = 0.1$ and a correlated flat Rayleigh channel with $f_D = 7$ Hz. First of all, note that for high Δ_{down} sizes the performance of both OLLA techniques is degraded, independently of the traffic load. However, while this degradation does not exceed the 4 % for the eOLLA, in the case of the traditional OLLA, this degradation varies between 5 and 10 %. Furthermore, given a Δ_{down} step size, the performance of the eOLLA does not vary with the traffic load. However, when using the traditional OLLA, low traffic load can degrade its performance with respect to the eOLLA up to 17 %. To sum up, the eOLLA outperforms the traditional OLLA while reducing the influence of the Δ_{down} step size and the traffic load.

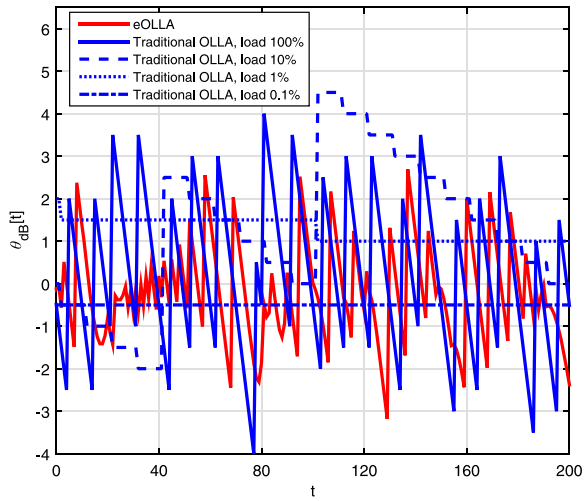

Fig. 7 Instantaneous offset comparison for a correlated flat Rayleigh channel ($f_D = 7$ Hz) with $\Delta_{down} = 0.5$ dB

4 eOLLA: application and simulation scenarios

The proposed eOLLA has been implemented in a complete 3GPP-LTE-A downlink simulator [10] in order to present realistic scenarios for which the eOLLA can significantly improve the performance of the traditional OLLA. These scenarios are based on LTE and LTE-A features. Both the traditional OLLA and the eOLLA have been evaluated for different sizes of Δ_{down}, all of them ensuring convergence according to Subsection 2.1.

4.1 Simulation environment

The 3GPP-LTE-A downlink simulator includes most of the features of physical (PHY) and medium access control (MAC) layers. Furthermore, it includes the LTE-A eICIC feature [16], which will be addressed in Subsection 4.5.

The MAC layer includes a hybrid automated repeat request (HARQ) process and an AMC process, which exchanges information with a channel aware scheduler. This scheduler allocates the LTE transport blocks (TBs) by assigning a set of physical resource blocks (PRBs) with a certain MCS [2] to each UE in order to meet some criteria.

At the BS, the PHY layer is made up of a coder system, which includes a CRC and a turbo coder; a quadrature amplitude modulation (QAM) mapper and an orthogonal frequency domain multiplexing (OFDM) modem. An AWGN channel and a multipath channel with temporal fading are included. At the UE, channel estimation and SINR estimation methods are implemented. With those methods, the channel state information (CSI) is reported to the BS [2]. The CSI is composed of the CQI, the precoding matrix indicator (PMI) and the rank indicator (RI). A QAM demapping and a channel-decoding process, which includes a CRC decoder and turbo decoder, is carried out to obtain the transmitted TBs. Finally, a HARQ entity manages the report of the ACK/NACK to the BS.

Table 6 summarizes the main simulation parameters. A typical pedestrian mobile speed (3 km/h) has been assumed to ensure the evaluation of the OLLA implementations under appropriate operating conditions of the AMC process. Regarding the channel aware scheduling, a round robin algorithm has been selected.

4.2 High traffic load with continuous transmission scenario

In this subsection, the performance of both the traditional OLLA and the eOLLA in a scenario with high

Table 5 Spectral efficiency (bps/Hz) comparison between traditional OLLA and eOLLA in correlated flat Rayleigh channel ($f_D = 7$ Hz)

	Load 100 %		Load 10 %		Load 1 %		Load 0.1 %	
Δ_{Down}	Traditional OLLA	eOLLA	Traditional OLLA	eOLLA	Traditional OLLA	eOLLA	Traditional OLLA	eOLLA
0.001 dB	2.43	2.45	0.24	0.245	0.0215	0.0245	0.0021	0.00245
0.01 dB	2.45	2.5	0.244	0.25	0.022	0.025	0.0021	0.0025
0.1 dB	2.41	2.4	0.23	0.24	0.021	0.024	0.0020	0.0024
0.5 dB	2.22	2.4	0.22	0.24	0.021	0.024	0.0020	0.0024

traffic load is evaluated . In this scenario, both algorithms update their offsets continuously as there will always be queued packets to be transmitted. Then, the benefit of eOLLA comes from its ability to dynamically adapt the size of the step, thus reducing the offset variance.

Next, main results for BLER, throughput, goodput, mean packet delay and jitter [17] are shown for different sizes of Δ_{down}. Except for the BLER, these results are expressed in percentage of the maximum value (which is also indicated in the figures). As shown in Fig. 8, there is no performance difference in terms of BLER since the $aBLER_T$ is met for both algorithms. However, it can be seen in Figs. 9 and 10 that a better performance in terms of throughput and goodput is achieved by the eOLLA for the majority of Δ_{down} sizes. Only for the lowest Δ_{down} sizes, throughput and goodput results are quite similar since the margin of adaptation of the step is very low. As the step size increases, the eOLLA gain is more remarkable, achieving a gain close to the 15 %.

Finally, the performance in terms of delay is evaluated, which is a very useful metric [18]. Figures 11 and 12 show the results for mean packet delay and jitter, respectively. In this case, the eOLLA also outperforms the traditional OLLA. While for the traditional OLLA, the optimum size of Δ_{down} is the lowest, the eOLLA tolerates higher sizes without a significant degradation of its performance.

4.3 High load traffic with bursty transmission scenario

In some scenarios, it is possible that some UEs cannot be served even if they have queued packets and good channel conditions, because of low-priority assignment or in case the BS is serving a great number of UEs. In this situation, the UE may stay in idle mode during long periods; as a consequence, channel conditions may change considerably during the time interval between packets, so the offset of the traditional OLLA would be outdated (since it can only be updated when an ACK/NACK is received). However, as analyzed in previous section, the eOLLA is

Table 6 Simulation parameters

Parameter	Value
Carrier frequency	2 GHz
Sampling frequency	7.68 MHz
System bandwidth	5 MHz
FFT size	512
Number of data subcarriers	300
OFDM symbols per subframe	14
Allocable PRBs	25
Channel model	Flat Rayleigh
Mobile terminal speed	3 km/h
Number of antennas	1 x 1
Channel aware scheduler algorithm	Round robin
Channel estimation method	Low-pass filter [21]
Interference and noise power estimation	Error-based
Reference signals overhead	According to 3GPP TS 36.211 [2]
Turbo decoder	SOVA-based
Number of CQI bits	4 [19]
Average SNR	15 dB
Δ_{down}	0.001–0.5 dB

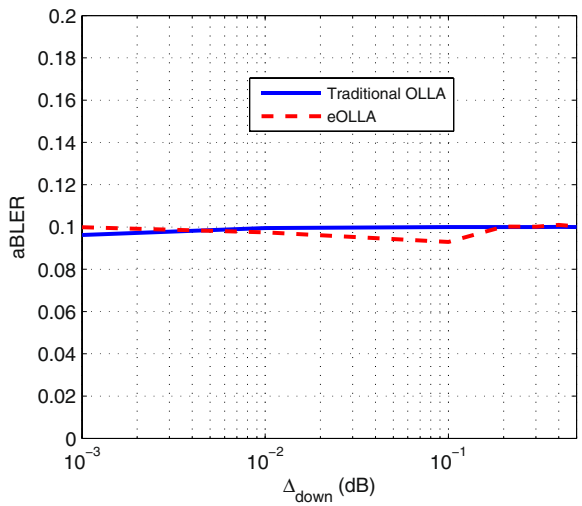

Fig. 8 BLER comparison for high traffic load with continuous transmission scenario

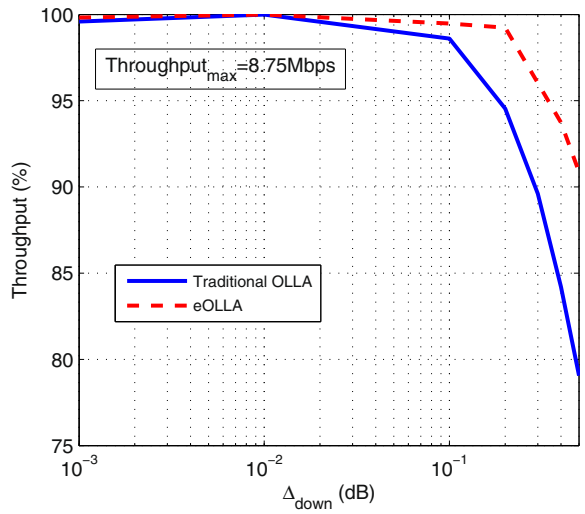

Fig. 9 Throughput comparison for high traffic load with continuous transmission scenario

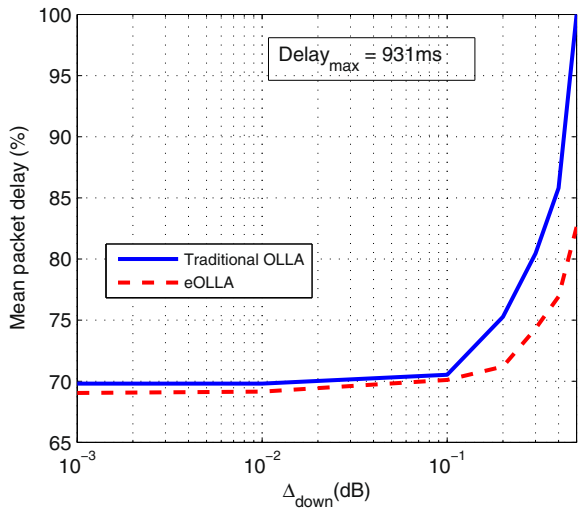

Fig. 11 Mean packet delay comparison for high traffic load with continuous transmission scenario

able to follow the channel variations even if no packets are received, since it uses the instantaneous SNR estimation to update its offset.

In this section, we evaluate a scenario where a data transmission is just allowed every 100 TTIs. Figures 13, 14, 15, 16, and 17 present the performance results in terms of throughput, goodput, mean packet delay, and jitter (expressed in percentage of the maximum value).

In Fig. 13, it can be seen that the traditional OLLA does not raise the $aBLER_T$ for the lowest values of Δ_{down}, whereas the eOLLA achieves the $aBLER_T$. The reason is that in the traditional OLLA, the offset cannot be updated continuously in order to follow the channel. As a result, Fig. 14 shows that for the lowest step sizes, the traditional OLLA decreases its throughput dramatically with respect to the eOLLA, as much as 15 %. Regarding the rest of performance metrics (Figs. 15, 16, and 17), the eOLLA generally outperforms the traditional OLLA while it is less influenced by the size of Δ_{down}. Only for the lowest values of Δ_{down}, delay metrics are pretty similar. However, since the $aBLER_T$ is

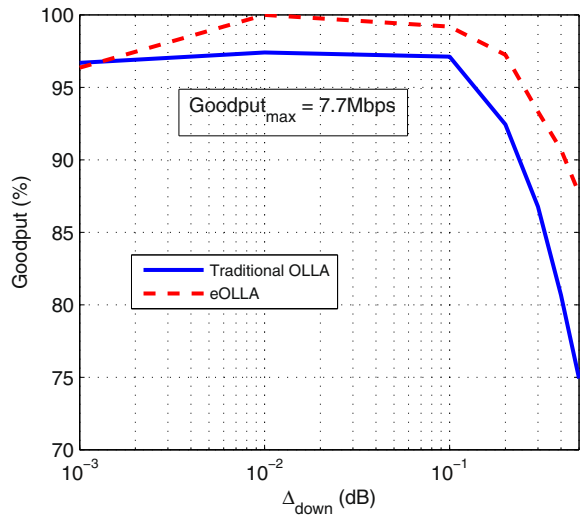

Fig. 10 Goodput comparison for high traffic load with continuous transmission scenario

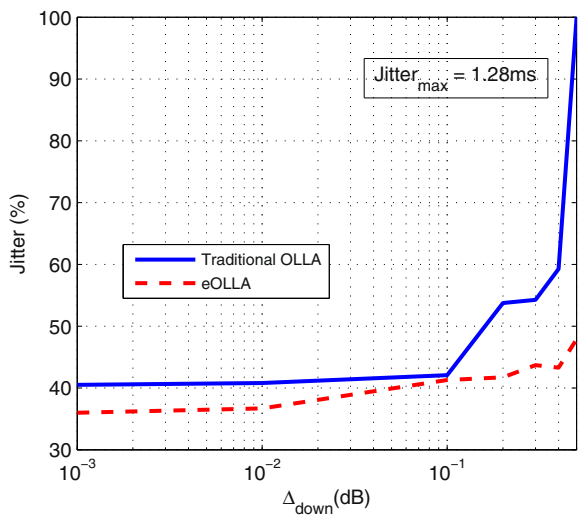

Fig. 12 Jitter comparison for high traffic load with continuous transmission scenario

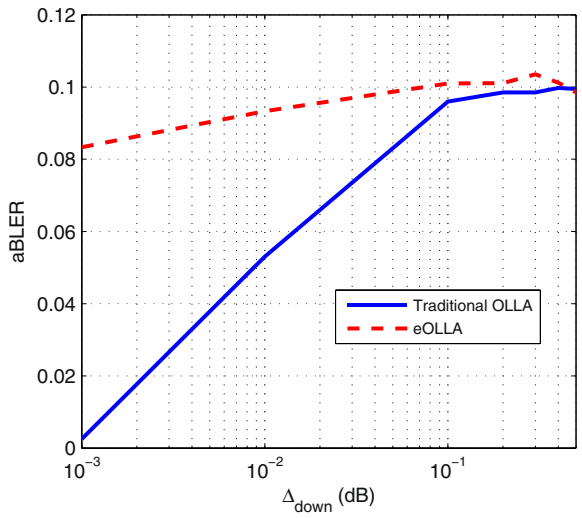

Fig. 13 BLER comparison for high traffic load with bursty transmission scenario

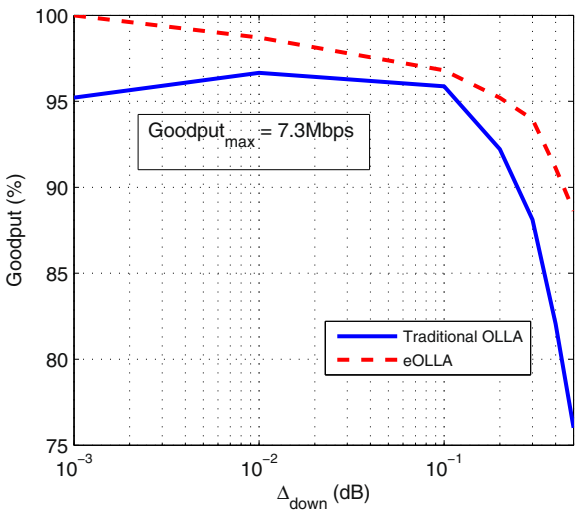

Fig. 15 Goodput comparison for high traffic load with bursty transmission scenario

not met for the traditional OLLA, these results are not meaningful.

4.4 Low-load traffic scenario

A M2M, online gaming [18] or an automated teller machine (ATM) scenario are examples of bursty traffic patterns with low data packet rates. In such scenarios, small data packets are exchanged over long periods of time; UE during these periods of time remain in idle mode. In LTE and LTE-A, there exists a minimum number of physical resources to allocate the TB to be transmitted [19]. For the DL, this number depends on the system bandwidth; for instance, for a system bandwidth of 5 MHz the minimum number of physical resources corresponds to one PRB. Thus, in case that the size of the packets to be transmitted is smaller than the minimum number of assignable physical resources, more redundancy will be included to fill them, i.e., the MCS will be modified making it more robust than the proposed by the reported CQI. As a consequence, less erroneous TBs will be received, and therefore, the aBLER will be lower than the $aBLER_T$, making the traditional OLLA to increase its offset in order to meet the target aBLER. Note that in this case, the traditional OLLA is unnecessarily

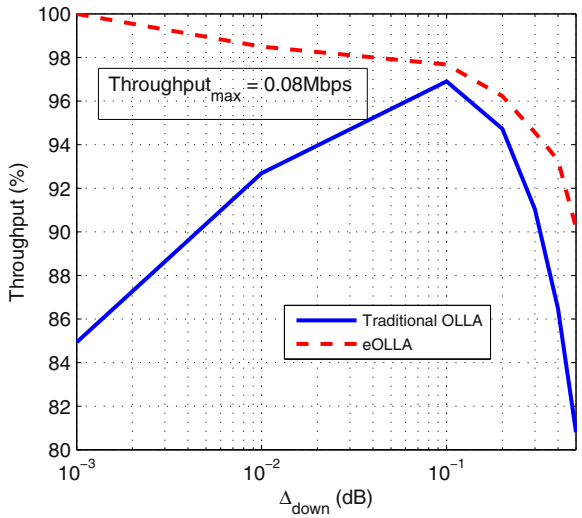

Fig. 14 Throughput comparison for high traffic load with bursty transmission scenario

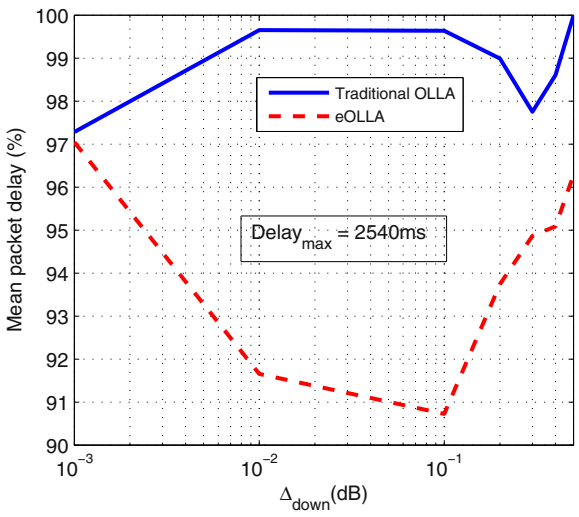

Fig. 16 Mean packet delay comparison for high traffic load with bursty transmission scenario

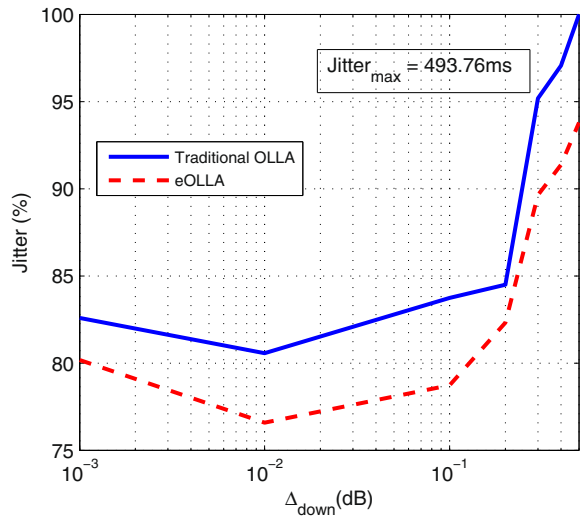

Fig. 17 Jitter comparison for high traffic load with bursty transmission scenario

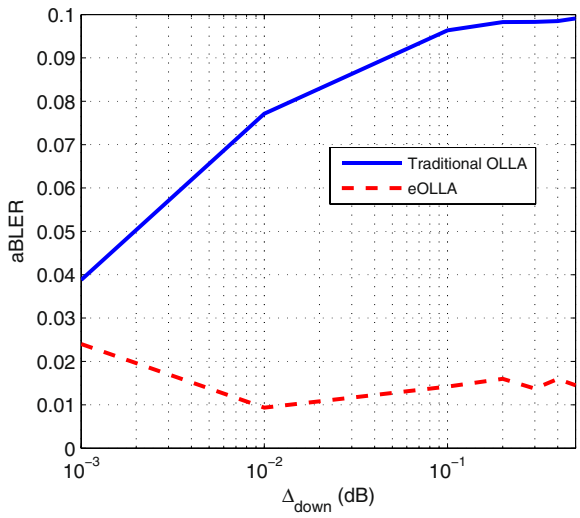

Fig. 18 BLER comparison for low load traffic scenario

forcing the aBLER to meet the target, since increasing the robustness of the MCS does not mean saving physical resources when the minimum number of assignable PRBs is used. Instead, it will cause erroneously received TB that could be avoided without increasing the amount of physical resources. Therefore, if the eOLLA is used in this scenario, since its offset is not affected by the number or erroneous TBs received but by the instantaneous channel state, it will not try to force the $aBLER_T$ to be met.

Next, the figures show the performance of the traditional OLLA and the eOLLA for an online gaming scenario [20], whose mean packet size is 70 bytes and mean period between packets is 50 ms. Figure 18 shows that the average BLER is not achieved for the eOLLA whereas the traditional OLLA achieves it for the majority of the Δ_{down} sizes. Regarding the normalized throughput, 100 % is always achieved since the capacity of the system is higher than the load of the traffic source. This fact also means that packet delay is always the minimum achievable value, i.e., 1 ms. Finally, goodput results of Fig. 19 show how the eOLLA outperforms significantly the traditional OLLA without any extra cost in terms of physical resources usage.

4.5 eICIC scenario

In LTE-A, the time domain-enhanced inter-cell interference coordination (eICIC) is defined as a technique to manage interference in heterogeneous networks (HetNets). An extensive description of this technique can be found in [16]. Briefly, in a scenario composed by a macro- and a pico-cell, a bias is applied to the coverage area of the pico-cell to balance the number of users associated to both types of cells. This process is named cell range expansion (CRE). Pico-cell users (PUEs) that are located in this CRE area generally suffer from very high interference from the macro-cell, since its transmission power is higher than the transmission power of the pico-cell. Thus, in order to improve the performance of these users, the macro-cell periodically does not schedule any transmission to their associated macro-cell users (MUEs), even if they have queued packets, generating the so called almost-blank subframes (ABSs). During the transmission of these ABSs, the pico-cell prioritizes the transmission to the PUEs of the CRE area

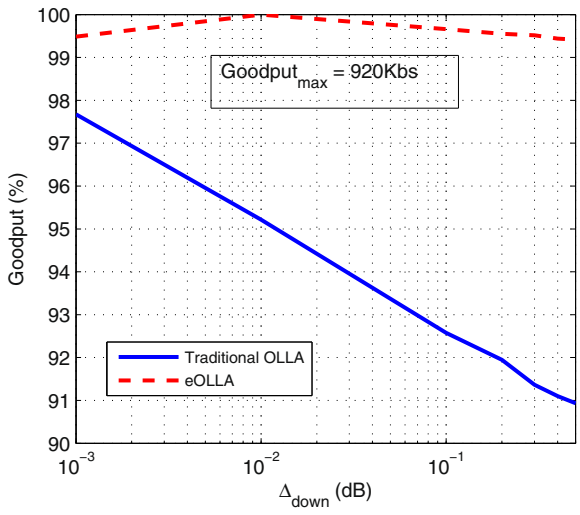

Fig. 19 Goodput comparison for low load traffic scenario

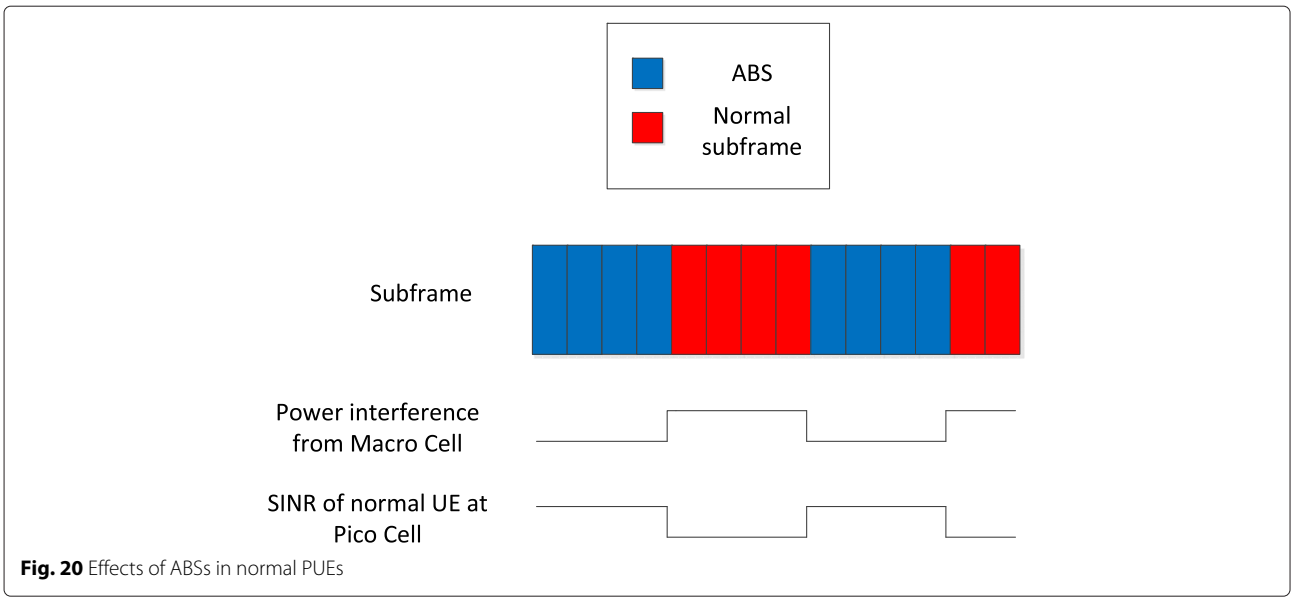

Fig. 20 Effects of ABSs in normal PUEs

since their SINR conditions improve significantly. On the other hand, during the transmission of normal subframes from the macro-cell, CRE PUEs are not scheduled by the pico-cell.

Thus, the eICIC technique implies that MUEs and CRE PUEs are not scheduled over certain periods of time (see Fig. 20). Therefore, in a similar way as the scenario described in Subsection 4.3, the offset of the traditional OLLA may not be able to follow the channel variations during these periods, while the eOLLA is.

Next, a performance comparison for both the traditional OLLA and the eOLLA is presented for a MUE and 30 ABSs transmitted every 40 TTIs. Note that this scenario is a mix of the two previously evaluated high-load traffic scenarios, since there is no continuous transmission, but the interval between transmissions is much lower than in the case of the high-load traffic with a bursty transmission scenario. Firstly, in Fig. 21, BLER results are presented for both algorithms, showing that the $aBLER_T$ is met in both cases. However, for the lowest size of Δ_{down}, the eOLLA is closer to the target than the traditional OLLA (which is consistent with results of subsection 4.3). Furthermore, in Figs. 22, 23, 24, and 25, it is shown how the proposed eOLLA also outperforms the traditional OLLA in terms of throughput, goodput, delay, and jitter, as much as a 10 %.

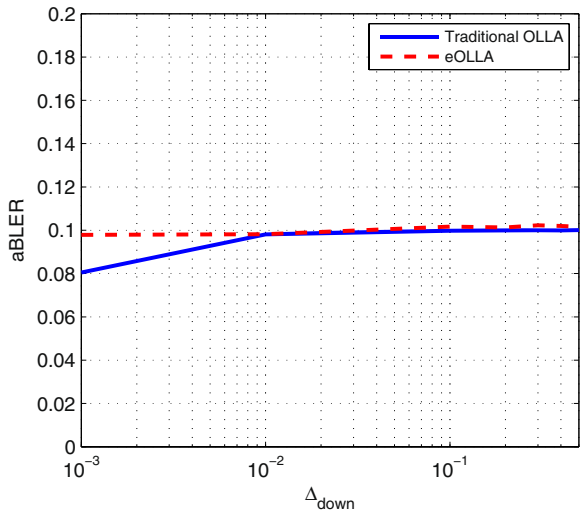

Fig. 21 BLER comparison for eICIC scenario

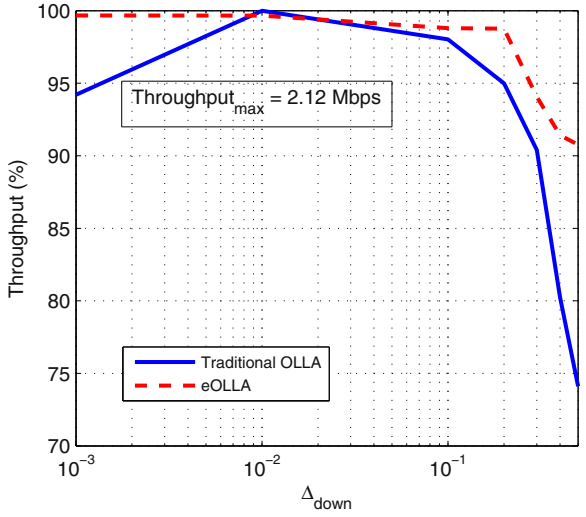

Fig. 22 Throughput comparison for eICIC scenario

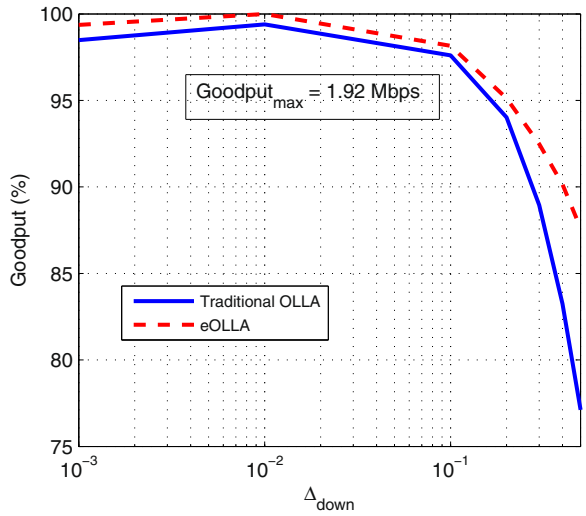

Fig. 23 Goodput comparison for eICIC scenario

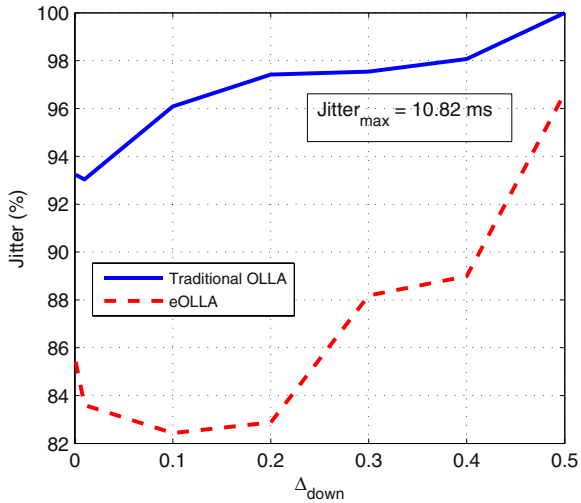

Fig. 25 Jitter comparison for eICIC scenario

A summary of the maximum gain of the proposed eOLLA with respect to the traditional OLLA for the different presented scenarios is shown in Table 7.

To sum up, the eOLLA outperforms the traditional OLLA in the whole set of evaluated scenarios. Then, for high-load traffic sources with continuous transmission, the ability of the eOLLA to adapt its step size is the cause of outperforming the traditional OLLA for the highest Δ_{down}. Regarding the bursty traffic sources, the ability of the eOLLA to follow the channel variations even if no packet is received is the key factor. Finally, for the eICIC scenario, a combination of both abilities are exploited. Regarding the size of Δ_{down}, previous results show that while for the traditional OLLA the selection of an appropriate value (which is different depending on the scenario) is crucial, for the eOLLA, there is a wide range of values that have a similar performance.

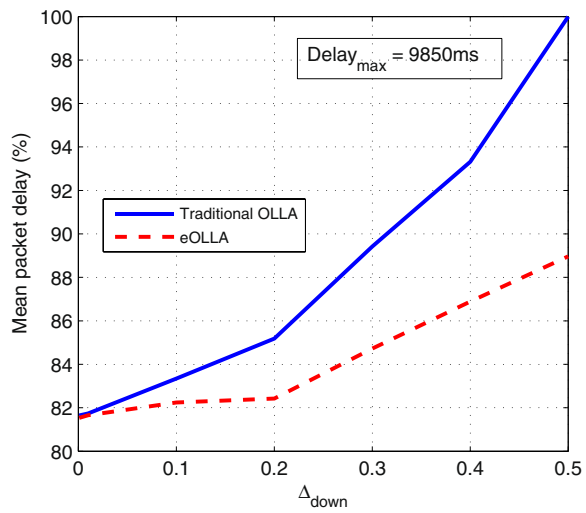

Fig. 24 Mean packet delay comparison for eICIC scenario

5 Conclusions

In this paper, the AMC process of LTE and LTE-A has been modeled in order to carry out a complete analysis of the well-known traditional OLLA algorithm. In particular, we present a model of the instantaneous BLER and the averaged BLER by means of binary logistic functions and modified binary logistic functions, respectively. Then, an expression to obtain the maximum step size of the traditional OLLA that ensures convergence has been presented. Furthermore, it has been studied how different sizes of this step lead to different performances depending on the specific scenario evaluated, even if they guarantee convergence. Next, a new approach to this algorithm, the enhanced OLLA (eOLLA), has been proposed based on logistic regression. This new algorithm outperforms the traditional OLLA since it is able to (1) dynamically adapt its step size according to the channel state and (2) update its offset value independently of whether a data packet has been received or not. Finally, a comparison of the performance of both algorithms has been carried out under different LTE and LTE-A scenarios, showing that the proposed eOLLA outperforms the traditional OLLA in all the cases.

Table 7 Summary of eOLLA maximum gain with respect to the traditional OLLA

Subsection	Throughput gain	Goodput gain	Mean packet delay gain	Jitter gain
High traffic load with continuous transmission scenario	15 %	17 %	17 %	52 %
High-load traffic with bursty transmission scenario	15 %	15 %	8 %	7 %
Low-load traffic scenario	NA	8 %	NA	NA
eICIC scenario	17 %	10 %	11 %	14 %

Competing interests
The authors declare that they have no competing interests.

Acknowledgements
This work has been partially supported by the Spanish Government and FEDER (TEC2013-44442-P).

Received: 9 September 2015 Accepted: 5 January 2016
Published online: 16 January 2016

References

1. ST Chung, AJ Goldsmith, Degrees of freedom in adaptive modulation: a unified view. IEEE Trans. Commun. **49**(9), 1561–1571 (2001). doi:10.1109/26.950343
2. 3GPP TS 36.211, *Evolved universal terrestrial radio access (E-UTRA); Physical Channels and Modulation (Release 10), V10.7.0*, (Sophia Antipolis Valbonne, France, 2013). http://www.3gpp.org/ftp/Specs/archive/36_series/36.211/36211-a70.zip
3. A Sampath, P Sarath Kumar, JM Holtzman, in *IEEE Vehicular Technology Conference*, vol. 2. On setting reverse link target sir in a cdma system, (1997), pp. 929–9332. doi:10.1109/VETEC.1997.600465
4. P Song, S Jin, in *International Conference on Communications and Information Technology (ICCIT)*. Performance evaluation on dynamic dual layer beamforming transmission in tdd lte system, (2013), pp. 269–274. doi:10.1109/ICCITechnology.2013.6579562
5. KI Pedersen, G Monghal, IZ Kovacs, TE Kolding, A Pokhariyal, F Frederiksen, *et al*, in *IEEE Vehicular Technology Conference (VTC Fall), Baltimore, USA*. Frequency domain scheduling for OFDMA with limited and noisy channel feedback, (2007), pp. 1792–1796. doi:10.1109/VETECF.2007.378
6. MG Sarret, D Catania, F Frederiksen, AF Cattoni, G Berardinelli, P Mogensen, in *21th European Wireless Conference, Budapest, Hungary*. Dynamic outer loop link adaptation for the 5G centimeter-wave concept, (2015), pp. 1–6
7. A Duran, M Toril, F Ruiz, A Mendo, Self-optimization algorithm for outer loop link adaptation in lte. IEEE Commun. Lett. **19**(11), 2005–2008 (2015). doi:10.1109/LCOMM.2015.2477084
8. J Ortin, P Garcia, F Gutierrez, A Valdovinos, Performance analysis of turbo decoding algorithms in wireless ofdm systems. IEEE Trans. Consum. Electron. **55**(3), 1149–1154 (2009). doi:10.1109/TCE.2009.5277969
9. A Agresti, *Categorical Data Analysis*. (John Wiley and Sons, Hoboken, New Jersey, 1990)
10. G Gómez, D Morales-Jiménez, JJ Sánchez-Sánchez, JT Entrambasaguas, A next generation wireless simulator based on MIMO-OFDM: LTE case study. EURASIP J. Wirel. Commun. Netw. **2010**, 15–11512 (2010)
11. 3GPP TS 36.212, *Evolved universal terrestrial radio access (E-UTRA); Multiplexing and Channel Coding (Release 10), V10.9.0*, (Sophia Antipolis Valbonne, France, 2015). http://www.3gpp.org/ftp/Specs/archive/36_series/36.212/36212-a90.zip
12. S Banach, *Sur les operations dans les ensembles abstraits et leur application aux equations integrales. PhD thesis*. (University of Lwow, Poland (now Ukraine), 1920)
13. 3GPP TS 36.304, *Evolved universal terrestrial radio access (E-UTRA); User Equipment (UE) Procedures in Idle Mode (Release 10), V10.8.0*, (Sophia Antipolis Valbonne, France, 2014). http://www.3gpp.org/ftp/Specs/archive/36_series/36.304/36304-a80.zip
14. RU Andrzej Cichocki, *Neural Networks for Optimization and Signal Processing*. (Wiley, Chichester, 1993)
15. A El-Koka, K-H Cha, D-K Kang, in *International Conference on Advanced Communication Technology (ICACT), PyeongChang, South Korea*. Regularization Parameter Tuning Optimization Approach in Logistic Regression, (2013), pp. 13–18
16. KI Pedersen, Y Wang, S Strzyz, F Frederiksen, Enhanced inter-cell interference coordination in co-channel multi-layer LTE-advanced networks. Wireless Commun. **20**(3), 120–127 (2013). doi:10.1109/MWC.2013.6549291
17. H Schulzrinne, S Casner, R Frederick, V Jacobson, RTP: a Transport Protocol for Real-time Applications, IETF RFC 3550 (2013). https://www.ietf.org/rfc/rfc3550.txt
18. IM Delgado-Luque, F Blanquez-Casado, MG Fuertes, G Gomez, MC Aguayo-Torres, JT Entrambasaguas, *et al*, in *European Signal Processing Conference (EUSIPCO), Bucharest, Romania*. Evaluation of latency-aware scheduling techniques for M2M traffic over LTE, (2012), pp. 989–993
19. 3GPP TS 36.213, *Evolved universal terrestrial radio access (E-UTRA); Physical Layer Procedures (Release 10), V10.13.0*, (Sophia Antipolis Valbonne, France, 2015). http://www.3gpp.org/ftp/Specs/archive/36_series/36.213/36213-ad0.zip
20. D Drajic, S Krco, I Tomic, P Svoboda, M Popovic, N Nikaein, N Zeljkovic, in *Conference on Wireless On-demand Network Systems and Services (WONS)*. Traffic generation application for simulating online games and m2m applications via wireless networks, (2012), pp. 167–174. doi:10.1109/WONS.2012.6152224
21. S Coleri, M Ergen, A Puri, A Bahai, Channel estimation techniques based on pilot arrangement in OFDM systems. IEEE Trans. Broadcast. **48**(3), 223–229 (2002). doi:10.1109/TBC.2002.804034